Cobalt(II) coordination polymers with 4'-substituted 4,2':6',4"- and 3,2':6',3"-terpyridines: engineering a switch from planar to undulating chains and sheets

Edwin C. Constable,* Catherine E. Housecroft,* Markus Neuburger, Srboljub Vujovic, Jennifer A. Zampese and Guoqi Zhang

Received (in XXX, XXX) Xth XXXXXXXXX 200X, Accepted Xth XXXXXXXXX 200X
First published on the web Xth XXXXXXXXX 200X
DOI: 10.1039/b000000x

Two new ligands 4'-(1*H*-imidazol-4-yl)-4,2':6',4"-terpyridine (**3**) and 4'-(4-dimethylaminophenyl)-3,2':6',3"-terpyridine (**4**) are described. Structure determination of **3**.$CHCl_3$ reveals the assembly of hydrogen-bonded chains of molecules of **3**; the preference for $NH_{imidazole}\cdots N_{tpy}$ over $NH_{imidazole}\cdots N_{imidazole}$ hydrogen bonds is consistent with the relative basicities of the heterocyclic rings. Reactions of $Co(NCS)_2$ with 4'-phenyl-4,2':6',4"-terpyridine (**1**), 4'-(4-ethynylphenyl)-4,2':6',4"-terpyridine (**2**) or **3**, produce two-dimensional networks. In each, the Co^{2+} ion is in an octahedral *trans*-$\{Co(N_{tpy})_4(NCS)_2\}$ environment. $[\{2Co(\mathbf{1})_2(NCS)_2{\cdot}5H_2O\}_n]$ and $[\{Co(\mathbf{3})_2(SCN)_2{\cdot}2MeOH\}_n]$ exhibit (4,4) nets. In $[\{Co(\mathbf{2})_2(NCS)_2{\cdot}0.67C_2H_4Cl_2{\cdot}MeOH{\cdot}H_2O\}_n]$, a (6,3) net is present. In all three coordination networks, there is substantial twisting of the 4,2':6',4"-terpyridine backbone and as a consequence, the dominant packing interactions are not the face-to-face π-stacking of tpy domains that are ubiquitous in many solid-state structures containing metal-bound tpy domains. As a preliminary investigation of the effects of altering the directionality of the donor set in the terpyridine domain, $Co(SCN)_2$ was reacted with ligand **4**, and the one-dimensional coordination polymer $[\{Co(\mathbf{4})(MeOH)_2(NCS)_2\}_n]$ was isolated. Ligand **4** adopts a *trans,trans*-arrangement and the zig-zag chains are undulating. The buckled sheets that result from the intermeshing of the chains contrast with the planar sheets observed in $[\{Cd(\mathbf{5})(OH_2)_2(ONO_2)(O_2NO){\cdot}H_2O\}_n]$ (**5** = 4'-(4-dimethylaminophenyl)-4,2':6',4"-terpyridine). The observed packing interactions suggest that the change from planar to undulating chains and sheets on going from the **5** to **4** is a consequence of optimizing face-to-face π-stacking interactions.

Introduction

The divergent 4,2':6',4"-terpyridine (4,2':6',4"-tpy) ligand is becoming popular as a building block for the assembly of coordination polymers and networks.[1-16] The ease with which the ligand synthesis can be adapted to introduce substituents at the 4'-position using Kröhnke,[17] one-pot or cascade strategies[18] allows facile engineering of the properties of the ligand and its complexes. Only the terminal pyridine rings of the tpy domain are involved in metal-binding (Scheme 1), and materials containing coordinated 4,2':6',4"-terpyridines have application as sensors for protons[6,7] and other Lewis acids. To date, zinc(II) has been commonly chosen as a node, either as a bent $\{ZnN_2X_2\}$ node (e.g. X = OAc, Cl, I)[1-23][4,7,11] or a linear $\{Zn_2N_2(\mu\text{-}OAc)_4\}$ node.[6,7] Both these are topologically the same. The reported examples indicate that one-dimensional polymers are favoured. However, the variation in zinc(II)/4'-substituted 4,2':6',4"-terpyridine structural motifs (metallohexacycles, polycatenated metallocapsules or one-dimensional chains) that can spontaneously arise illustrates that we are far from understanding the assembly process, and as a consequence, controlling it.[15] Subtleties of crystallization conditions apart, the structural diversity in complexes of terpyridines depends upon the N,N',N"-substitution pattern in the tpy ligand (48 possible isomers) and the coordination geometry at the metal ion. In this paper, we focus on an octahedral cobalt(II) centre which functions as a linear node for network assembly. We describe the reactions of $Co(SCN)_2$ with three 4'-substituted 4,2':6',4"-tpy ligands (**1**-**3**, Scheme 1) and one 4'-substituted 3,2':6',3"-terpyridine (3,2':6',3"-tpy) ligand **4** (Scheme 1). Both peripheral *N,N'*-donor sets are divergent, and both could subtend a 120° angle (Scheme 2). However, whereas rotations about the inter-ring C–C bonds in 4,2':6',4"-tpy have no effect on the directionalities of the peripheral *N*-donors, rotations about the corresponding C–C bonds in 3,2':6',3"-tpy lead to different ligand conformations, three of which are shown in Scheme 2. The coordination chemistry of 3,2':6',3"-tpy and its derivatives is little explored. Granifo and coworkers have reported that 4'-phenyl-3,2':6',3"-tpy, **5**, reacts with $Zn(OAc)_2$ to yield the discrete, dinuclear complex $[(AcO\text{-}\kappa O,O')_2Zn(\mu\text{-}\mathbf{5})Zn(AcO\text{-}\kappa O,O')_2]{\cdot}H_2O$ in which the water molecule is hydrogen-bonded between the two $\{Zn(AcO\text{-}\kappa O,O')_2\}$ domains.[19] To the best of our knowledge, only three coordination polymers based on 3,2':6',3"-tpy metal-binding domains have been structurally characterized[20,21] and all contain 4'-(4-pyridyl)-3,2':6',3"-tpy in which the central N-donor of the tpy unit remains uncoordinated.[22,23]

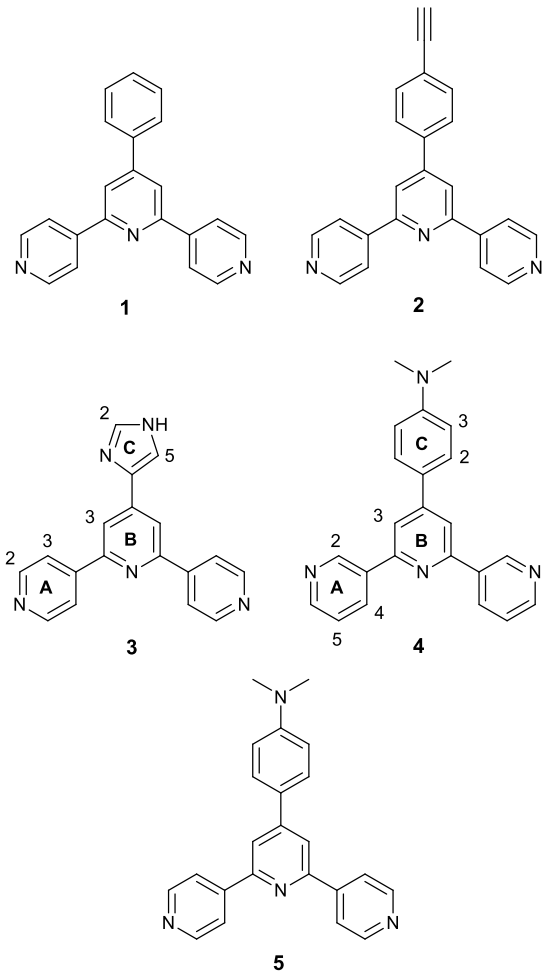

Scheme 1. Structures of ligands **1**-**5** showing atom labelling for NMR spectroscopic assignments.

Experimental

^{1}H and ^{13}C NMR spectra were recorded on a DRX-500 NMR spectrometer (chemical shifts referenced to residual solvent peaks, TMS = δ 0 ppm). Infrared spectra of solid samples were recorded on a Shimadzu FTIR-8400S spectrophotometer with a Golden Gate diamond ATR accessory. Electrospray ionization mass spectra were recorded on a Bruker esquire 3000plus mass spectrometers.

Ligands **1** and **2** were prepared as previously reported.[1,8]

Ligand 3

4-Acetylpyridine (2.42 g, 20.0 mmol) was added to a solution of 1*H*-imidazole-4-carbaldehyde (0.960 g, 10.0 mmol) in EtOH (40 cm^3). KOH pellets (1.12 g, 20 mmol) were added, followed by aqueous NH_3 (32%, 40 cm^3). The resulting orange solution was stirred at room temperature for 16 h, after which time, aqueous $NaHCO_3$ was added. The suspension was stirred for 10 min and then filtered. The product was washed with H_2O and EtOH and dried *in vacuo* over P_2O_5. Compound **3** was isolated as a white solid (1.20 g, 40.1%). m.p. > 300°C. ^{1}H NMR (500 MHz, $CDCl_3/CD_3OD$) δ / ppm) 8.50 (d, J = 5.2 Hz, 4H, H^{A2}), 8.11 (s, 2H, H^{B3}), 7.99 (d, J = 5.2 Hz, 4H, H^{A3}), 7.61 (s, 1H, H^{C2}), 7.57 (s, 1H, H^{C5}); ^{13}C NMR (126 MHz, $CDCl_3/CD_3OD$) δ / ppm 154.5 (C^{A4}), 149.5 (C^{B4}), 149.3 (C^{A2}), 146.9 (C^{A4}), 136.8 ($C^{C2/C4}$), 136.75 ($C^{C2/C4}$), 121.4 (C^{A3}), 116.5 (C^{B3}), 115.4 (C^{C5}). IR (solid, cm^{-1}) ν 3087br, 2851br, 2675w, 1596s, 1558s, 1458s, 1424m, 1307w, 1175m, 1124w, 1084w, 1062m, 1004m, 959m, 921w, 897w, 826s, 785m, 739m, 668s, 655s, 633s. ESI-MS *m/z* 621.1 [2M + Na]$^+$ (calc. 621.2), 322.1 [M + Na]$^+$ (base peak, calc. 322.1), 300.2 [M + H]$^+$ (calc. 300.1). Found C 71.36, H 4.56, N 22.90; $C_{18}H_{13}N_5 \cdot 0.2H_2O$ requires C 71.37, H 4.46, N 23.12%.

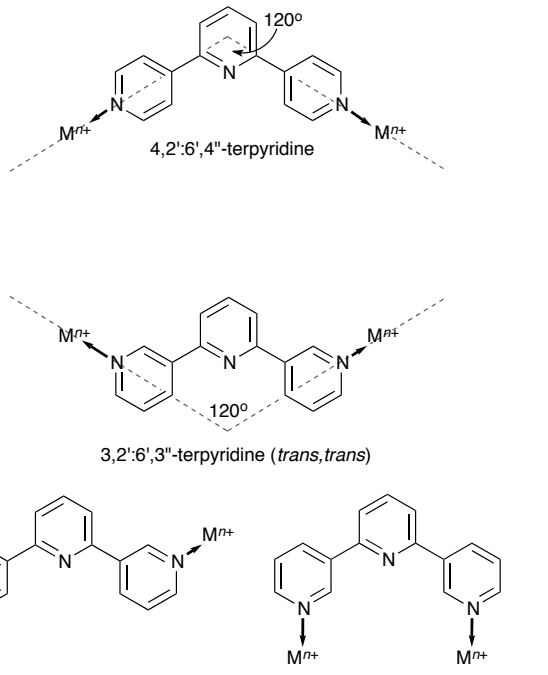

Scheme 2. Divergent binding mode of 4,2':6',4"-tpy, compared to possible binding modes of 3,2':6',3"-tpy.

Ligand 4

3-Acetylpyridine (1.45 g, 12.0 mmol) was added to a solution of 4-dimethylaminobenzaldehyde (0.89 g, 6.0 mmol) in EtOH (20 cm^3). KOH pellets (0.67 g, 12 mmol) were added to the reaction mixture, followed by aqueous NH_3 (32%, 20 cm^3). The resulting orange solution was stirred at room temperature for 18 h, during which time a yellow suspension formed. The solid was collected by filtration, washed well with H_2O and EtOH and dried *in vacuo* over P_2O_5. Compound **4** was isolated as a yellow solid (1.25 g, 59.2%). m.p. 112-113 °C. ^{1}H NMR (500 MHz, $CDCl_3$) δ 9.34 (s, 2H, H^{A2}), 8.66 (d, J = 4.4 Hz, 2H, H^{A6}), 8.47 (d, J = 7.9 Hz, 2H, H^{A4}), 7.89 (s, 2H, H^{B3}), 7.66 (d_{AB}, J = 8.7 Hz, 2H, H^{C2}), 7.42 (m, 2H, H^{A5}), 6.81 (d_{AB}, J = 8.8 Hz, 2H, H^{C3}), 3.03 (s, 6H, H^{Me}). ^{13}C NMR (126 MHz, $CDCl_3$) δ/ ppm 155.3 (C^{B2}), 151.5 (C^{C4}), 150.7 (C^{B4}), 150.2 (C^{A6}), 148.6 (C^{A2}), 135.3 (C^{A3}), 134.7 (C^{A4}), 128.0 (C^{C2}), 125.1 (C^{C1}), 123.8 (C^{A5}), 116.6 (C^{B3}), 112.7 (C^{C3}), 40.5 (C^{Me}). IR (solid, cm^{-1}) ν 1598s, 1520s, 1447w, 1430w, 1417w, 1357m, 1233w, 1199m, 1172w, 1025m, 946w, 875w, 802s, 730s. ESI-MS *m/z* 727.4 [2M + Na]$^+$ (base peak, calc.727.3), 375.2 [M + Na]$^+$ (calc. 375.2), 353.2 [M + H$^+$] (calc. 353.2). Found C 77.00, H 5.79, N 15.37; $C_{23}H_{20}N_4 \cdot 0.3H_2O$ requires C

77.20, H 5.80, N 15.66%.

[{2Co(1)$_2$(NCS)$_2$·5H$_2$O}$_n$]

A solution of **1** (15.5 mg, 0.0500 mmol) in MeOH/1,2-$Cl_2C_6H_4$ (10 cm^3, 1 : 4, v/v) was placed in a test tube. A mixture of MeOH and 1,2-$Cl_2C_6H_4$ (5 cm^3, 1 : 1, v/v) was layered on the top of this solution, followed by a solution of $Co(SCN)_2$ (8.75 mg, 0.0500 mmol) in MeOH (10 cm^3). The tube was sealed and allowed to stand at room temperature for one month, during which time X-ray quality orange blocks grew on the walls of the tube. The crystals were collected by decanting the solvent and were washed with MeOH and dried in air. Yield: 13.1 mg (62.5% based on **1**). IR (solid, ν, cm^{-1}) 2058s, 1657m, 1598s, 1560s, 1540s, 1510m, 1398m, 1215w, 1063w, 1015w, 835s, 764s, 689s, 668s, 646s. Found C 63.85, H 4.23, N 13.45; $C_{44}H_{30}CoN_8S_2$·2.5H_2O requires C 63.00, H 4.21, N 13.36%.

[{Co(2)$_2$(NCS)$_2$·0.67$C_2H_4Cl_2$·MeOH·H_2O}$_n$]

A solution of **2** (33.3 mg, 0.100 mmol) in MeOH/1,2-$Cl_2C_6H_4$ (10 cm^3, 1 : 4, v/v) was placed in a test tube, and a mixture of MeOH and 1,2-$C_2H_4Cl_2$ (5 cm^3, 1 : 1, v/v) was layered on the top. Finally, a solution of $Co(SCN)_2$ (17.5 mg, 0.100 mmol) in MeOH (10 cm^3) was layered on the top of the second layer. The tube was sealed and allowed to stand at room temperature for a month, during which time X-ray quality pink blocks grew on the walls of the tube. The product was isolated by decanting the solvent and was washed with MeOH, and dried in air. Yield: 29.8 mg (62.3% based on **2**). IR (solid, ν, cm^{-1}) 3278s, 3215w, 2066s, 1598s, 1570m, 1539s, 1510m, 1397m, 1215m, 1064m, 1014s, 853w, 825s, 673s, 649s, 638s. Found C 63.81, H 3.89, N 12.07; $C_{48}H_{30}CoN_8S_2$·0.67$C_2H_4Cl_2$·MeOH·H_2O requires C 63.10, H 4.07, N 11.69%.

[{Co(3)$_2$(NCS)$_2$·2MeOH}$_n$]

A solution of **3** (29.9 mg, 0.100 mmol) in MeOH/1,2-$Cl_2C_6H_4$ (10 cm^3, 1 : 4, v/v) was placed in a test tube, and a mixture of MeOH and 1,2-$Cl_2C_6H_4$ (5 cm^3, 1 : 1, v/v) was layered over the first solution, followed by a layer of a solution of $Co(SCN)_2$ (35.0 mg, 0.200 mmol) in MeOH (10 cm^3). The tube was sealed and left to stand at room temperature for a month. During this period, X-ray quality brown needles formed on the walls of the tube. Crystals were collected by decanting the solvent, were washed with MeOH, and dried in air. Yield: 31.2 mg (74.5% based on **3**). IR (solid, ν, cm^{-1}) 2070s, 1657s, 1604s, 1560m, 1510m, 1458m, 1214w, 1014m, 836s, 668s, 642m. Found C 54.07, H 4.07, N 19.22; $C_{38}H_{26}CoN_{12}S_2$·MeOH·3H_2O requires C 54.48, H 4.22, N 19.55% (see text).

[{Co(4)(MeOH)$_2$(NCS)$_2$}$_n$]

A solution of **4** (17.6 mg, 0.0500 mmol) in MeOH/1,2-$Cl_2C_6H_4$ (10 cm^3, 1 : 4, v/v) was placed in a test tube, and a mixture of MeOH and 1,2-$Cl_2C_6H_4$ (5 cm^3, 1 : 1, v/v) was layered on top. A final layer of a solution of $Co(SCN)_2$ (8.75 mg, 0.050 mmol) in MeOH (10 cm^3) was added carefully. The tube was sealed and left to stand at room temperature for a month, during which time X-ray quality orange blocks formed on the glass walls. The crystals were isolated by decanting the solvent and were washed with MeOH, and dried in air. Yield: 23.0 mg (77.8%). IR (solid, ν, cm^{-1}) 3234br, 2087s, 1595s, 1576m, 1533s, 1481w, 1388m, 1361m, 1215w, 1193w, 1170w, 1055w, 1033w, 1014s, 950w, 885w, 809s, 702s. Found C 54.76, H 4.74, N 13.72; $C_{27}H_{28}CoN_6O_2S_2$·0.33H_2O requires C 54.27, H 4.83, N 14.06%.

Table 1 Crystallographic data for **3**·$CHCl_3$, [{2Co(**1**)$_2$(NCS)$_2$·5H_2O}$_n$], [{Co(**2**)$_2$(NCS)$_2$·0.67$C_2H_4Cl_2$·MeOH·H_2O}$_n$], [{Co(**3**)$_2$(NCS)$_2$·2MeOH}$_n$] and [{Co(**4**)(MeOH)$_2$(NCS)$_2$}$_n$].

Compound	**3**·$CHCl_3$	[{2Co(**1**)$_2$(NCS)$_2$·5H_2O}$_n$]	[{Co(**2**)$_2$(NCS)$_2$·0.67$C_2H_4Cl_2$·MeOH·H_2O}$_n$]	[{Co(**3**)$_2$(NCS)$_2$·2MeOH}$_n$]	[{Co(**4**)(MeOH)$_2$(NCS)$_2$}$_n$]
Formula	$C_{18}H_{13}N_5$·$CHCl_3$	$C_{88}H_{70}Co_2N_{16}O_5S_4$	$C_{50.33}H_{38.67}Cl_{1.33}CoN_8O_2S_2$	$C_{40}H_{34}CoN_{12}O_2S_2$	$C_{27}H_{28}CoN_6O_2S_2$
Formula weight	418.70	1677.72	957.90	837.85	591.62
Crystal colour and habit	colourless block	orange block	pink block	brown needle	orange block
Crystal system	monoclinic	monoclinic	monoclinic	monoclinic	orthorhombic
Space group	$P2_1/c$	$C2/c$	$C2/c$	$P2_1/c$	$Pbca$
a, b, c / Å	7.0576(8) 21.727(3) 12.0929(12)	24.608(2) 10.6168(10) 17.7748(16)	28.199(6) 10.371(2) 32.295(7)	23.3334(7) 10.3868(3) 17.3827(6)	14.3014(8) 14.3112(7) 26.2091(12)
β / °	103.978(8)	116.118(6)	103.51(3)	109.477(2)	90
U / Å^3	1799.5(4)	4169.7(6)	9184(3)	3971.8(2)	5364.2(5)
D_c / Mg m^{-3}	1.546	1.328	1.383	1.401	1.465
Z	4	2	8	4	8
μ(Mo-K$_\alpha$) / mm^{-1}	0.524	0.560	0.593	0.590	0.833
T / K	173	173	173	123	173
Refln. collected	29140	45214	81174	102487	139949
Unique refln. (R_{int})	4014 (0. 0611)	3715 (0. 0647)	10540 (0.0426)	17451 (0.056)	6116 (0.0591)
Refln. for refinement	3531	3582	9902	12290	5980
Parameters	244	274	615	678	353
Threshold	$I>2\sigma(I)$	$I>2\sigma(I)$	$I>2\sigma(I)$	$I>2\sigma(I)$	$I>2\sigma(I)$
*R*1 (*R*1 all data)	0.0368 (0.0437)	0.0581 (0.0597)	0.0463 (0.0487)	0.0697 (0.1092)	0.0415 (0.0425)
*wR*2 (*wR*2 all data)	0.0894 (0.0931)	0.1598 (0.1612)	0.1244 (0.1264)	0.0669 (0.1443)	0.0928 (0.0933)
Goodness of fit	1.054	1.119	1.043	1.0536	1.216

Crystallography

Data were collected on a Bruker-Nonius KappaAPEX diffractometer, with data reduction, solution and refinement using the programs APEX2[24], SIR92[25] and CRYSTALS,[26] or on a Stoe IPDS diffractometer with data reduction, solution and refinement using Stoe IPDS software[27] and SHELXL97.[28] Ortep figures were drawn using Ortep-3 for Windows,[29] and Mercury v. 2.3 and 2.4[30,31] were used to analyse the structures. See Table 1 for crystallographic data.

Results and discussion

Ligand synthesis and charcterization

Ligands **3** and **4** were prepared in moderate yields by treatment of 4-acetylpyridine with 1*H*-imidazole-4-carbaldehyde or 3-acetylpyridine with 4-dimethylaminobenzaldehyde in the presence of KOH followed by addition of aqueous NH_3. The electrospray mass spectrum of each compound exhibited peaks corresponding to $[2M + Na]^+$, $[M + Na]^+$ and $[M + H]^+$. Solution ($CDCl_3$) ^1H and ^{13}C NMR spectra were fully assigned with the aid of COSY, NOESY, DEPT, HMBC and HMQC techniques, and were consistent with a symmetrical tpy domain. AB-Pattern doublets at δ 8.55 and 7.99 ppm for protons H^{A2} and H^{A3} in **3** (Scheme 1) are replaced by signals at δ 9.34, 8.66, 8.47 and 7.42 pm for H^{A2}, H^{A6}, H^{A4} and H^{A5} in **4**. The change from the 4'-imidazolyl to 4'-(4-*N,N*-dimethylamino)phenyl substituent results in a shift in the singlet for H^{B3} from δ 8.11 ppm in **3** to δ 7.89 ppm in **4**. In the ^{13}C NMR spectrum of **3**, the signal for C^{C5} was poorly resolved and a chemical shift of δ 115.4 ppm was confirmed from a crosspeak in the HMQC spectrum.

Crystals of **3**·$CHCl_3$ were grown from a chloroform/methanol solution of the compound by slow evaporation. The molecular structure of **3** is illustrated in Fig. 1a, with selected bond distances and angles listed in the caption. Three of the rings in the ligand are essentially coplanar, while the pyridine ring containing N1 exhibits a greater deviation from the plane; the angles between the least squares planes of the rings containing N1/N2, N2/N3 and N2/N4 are 17.42(8), 6.93(8) and 5.34(9)°. The twisting of the N1-containing ring is associated with the crystal packing: chloroform molecules reside in pockets between pairs of the N1-containing pyridine units of adjacent ligands (Fig. 1b). The relative basicities of the pyridine and imidazole moieties in **3** can be estimated from values of pK_b of 4-phenylpyridine (8.56) and of 4-phenylimidazole (7.90).[32] From the difference in pK_b values, one predicts that $NH_{imidazole}...N_{pyridine}$ hydrogen bonding should be preferred over $NH_{imidazole}...N_{imidazole}$ hydrogen bond formation. Indeed, this is observed in the solid state structure of 4-(5-(4-fluorophenyl)-1*H*-imidazol-4-yl)pyridine.[33] The pK_a of 4-phenylimidiazole is 13.42,[32] suggesting that complete transfer of H^+ from the imidazole to pyridine domain will not occur. The solid-state structure of **3** is consistent with these predictions: chains of molecules assemble (Fig. 1b) supported by $NH_{imidazole}...N3_{pyridine}$ hydrogen-bonds (Table 2). The chains are connected into sheets through weak CH...N and CH...Cl contacts (Table 2). The overall lattice consists of a layer assembly and face-to-face π-stacking is a dominant contribution to the packing interactions. Centrosymmetric pairs of tpy domains engage in face-to-face π-stacking at a separation of 3.5 Å; the distance between the centroids of the pyridine rings containing atoms N2 and $N3^{iv}$ (symmetry code iv = $-x$, $1 - y$, $2 - z$) is 3.9 Å.[34]

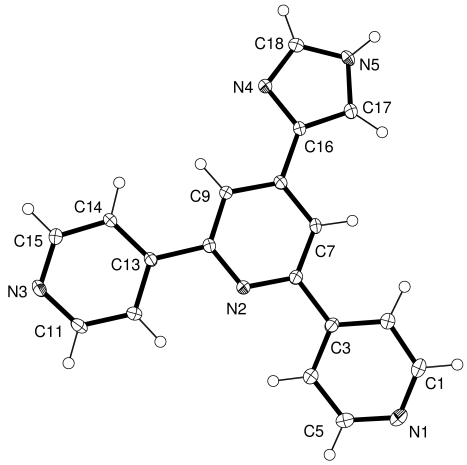

(a)

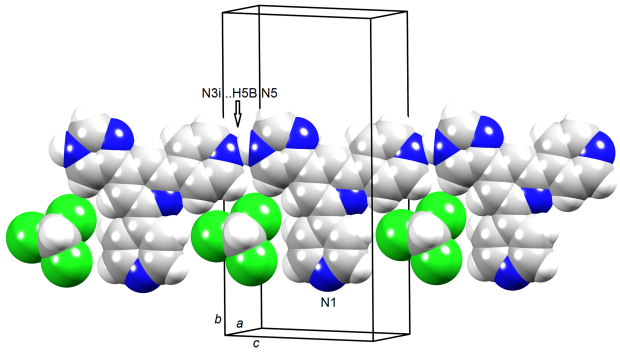

(b)

Fig. 1. (a) Structure of **3** in **3**·$CHCl_3$ (ellipsoids plotted at 40% probability level). Selected bond parameters: N1-C1 = 1.326(2), N1-C5 = 1.331(2), N2-C10 = 1.3346(19), N2-C6 = 1.3392(19), N3-C15 = 1.329(2), N3-C11 = 1.333(2) C16-C17 = 1.364(2), C16-N4 = 1.3764(19), C17-N5 = 1.357(2), C18-N4 = 1.313(2), C18-N5 = 1.340(2) Å; C17-C16-N4 = 109.27(13), N5-C17-C16 = 106.68(13), C18-N4-C16 = 104.82(13), C18-N5-C17 = 106.60(13), N4-C18-N5 = 112.62(14)°. (b) Chains of hydrogen-bonded molecules of **3** and location of $CHCl_3$ solvent molecules between N1-containing pyridine rings.

Table 2. Intermolecular contacts in **3**·$CHCl_3$. The symmetry code refers to the atom with the asterisk

D–H…A	H…A / Å	D…A / Å	D-H…A / °	Symmetry code
N5H5B...N3*	2.00	2.8473(19)	162	$-1 + x, y, -1 + z$
C14H14A...N1*	2.57	3.482(2)	160	$-x, {}^1/_2 + y, {}^3/_2 - z$
C15H15A...Cl*	2.67	3.5385(19)	152	$x, {}^3/_2 - y, {}^1/_2 + z$

$[\{2Co(1)_2(NCS)_2 \cdot 5H_2O\}_n]$

Given the extended π-system in **1**, it is not surprising that face-to-face π-interactions[34,35,36] feature significantly in the solid state packing of coordination polymers and networks of complexes containing **1** or 4'-(4-X-C_6H_4) (X = Me, Et, C≡CH,

Br, SMe, NMe_2) derivatives.[3,4,5,6,7,8] Reaction of **1** with $Co(NCS)_2$ resulted in the growth of crystals of $[\{2Co(\mathbf{1})_2(NCS)_2{\cdot}5H_2O\}_n]$, and elemental analytical data were consistent with the crystal chosen for X-ray diffraction being representative of the bulk sample. Figure 2a depicts the contents of the asymmetric unit to provide the atom labelling scheme for $[\{2Co(\mathbf{1})_2(NCS)_2{\cdot}5H_2O\}_n]$. Atom Co1 is in an octahedral CoN_6-environment (Fig. 2b), being located on the inversion centre (0, 1, $^1/_2$) of space group $C2/c$ (Wyckoff position *a*). The N-Co-N bond angles lie in the range 88.61(10) to 91.39(10)°. Ligand **1** coordinates through atoms N1 and N3, bridging Co1 and Co1^{i} (symmetry code i = $-^1/_2 - x$, $^1/_2 + y$, $^1/_2 - z$); atom N2 remains uncoordinated. Symmetry related ligands connect Co1 to Co1^{ii}, Co^{iii} and Co^{iv} (symmetry codes ii = $^1/_2 - x$, $^1/_2 + y$, $^3/_2 - z$; iii = $-^1/_2 - x$, $-^1/_2 + y$, $^1/_2 - z$; iv = $^1/_2 - x$, $-^1/_2 + y$, $^3/_2 - z$). Extension of these connectivities leads to the propagation of a two-dimensional network consisting of interconnected [4 + 4] metallomacrocyclic motifs (Fig. 3). The (4,4) net mimics that observed in $[\{Cd(\mathbf{1})_2(ONO_2)_2{\cdot}MeOH{\cdot}CHCl_3\}_n]$.[1]

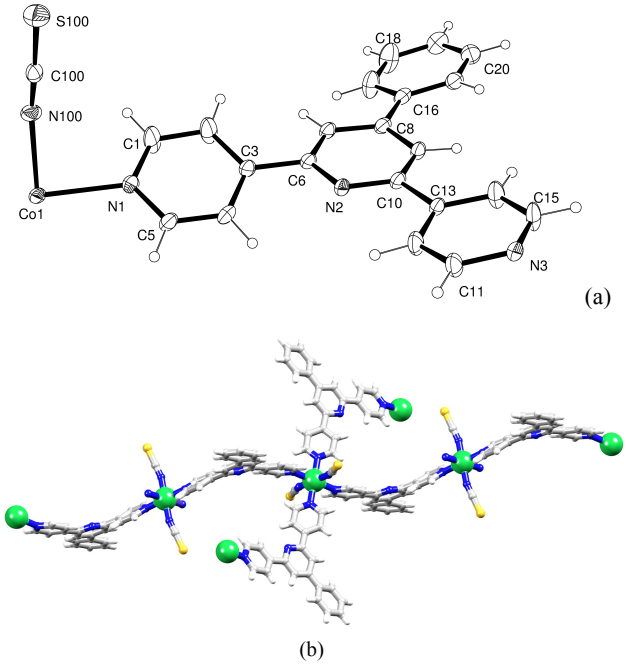

Fig. 2. (a) The asymmetric unit in $[\{2Co(\mathbf{1})_2(NCS)_2{\cdot}5H_2O\}_n]$ (ellipsoids plotted at 30% probability level, and solvent molecules excluded). Selected bond parameters: Co1-N1 = 2.186(3), Co1-N100 = 2.065(3), N100-C100 = 1.156(4), S100-C100 = 1.624(4) Å; C100-N100-Co1 = 160.4(2)°. (b) Octahedral coordination environment around atom Co1 (green).

The tpy unit of coordinated ligand **1** is highly twisted, with angles of 26.72(19) and 13.83(17)° between the least squares planes of the rings containing pairs of atoms N1/N2 and N2/N3. This deformation gives rise to the undulating structural motifs evident in Fig. 2b. The phenyl ring of ligand **1** is twisted 15.45(19)° out of the plane of the pyridine (py) ring to which it is attached. Despite the non-planarity of the phenylpyridine unit, centrosymmetric pairs of phenylpyridine domains in adjacent sheets engage in face-to-face π-interactions, with the separation of planes between rings containing C16 and C16^{v} being 3.15 Å (symmetry code v = $^3/_2 - x$, $^3/_2 - y$, $1 - z$), and the distance between the centroids of rings containing C16 and N2^{v} being 3.94 Å.[34] Figure 4 illustrates two such stacking interactions between parts of three adjacent sheets. Since there is only one independent ligand in the asymmetric unit, all phenylpyridine entities are involved in stacking interactions and are responsible for locking the two-dimensional coordination networks together in the crystal lattice. One and a half water molecules are disordered within a void in the asymmetric unit, and have been modelled as half occupancy oxygen atoms over three positions (the H atoms could not be located).

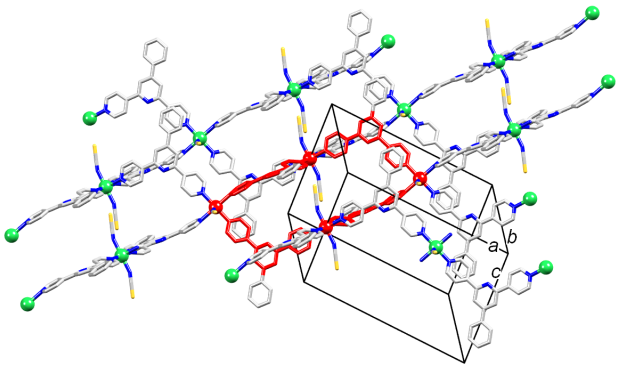

Fig. 3. Part of one sheet in $[\{2Co(\mathbf{1})_2(NCS)_2{\cdot}5H_2O\}_n]$ with one [4 + 4] metallomacrocyclic building block depicted in red. Co atoms are shown in ball representation.

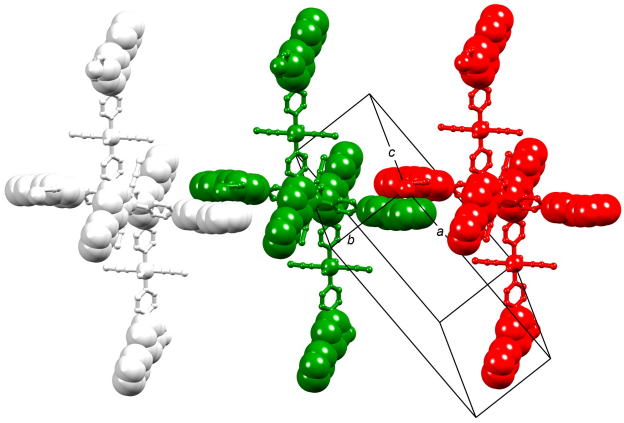

Fig. 4. Face-to-face π-stacking of pairs of phenylpyridine units between adjacent sheets in $[\{2Co(\mathbf{1})_2(NCS)_2{\cdot}5H_2O\}_n]$ (see text). Phenylpyridine units are shown in space-filling representation.

$[\{Co(\mathbf{2})_2(NCS)_2{\cdot}0.67C_2H_4Cl_2{\cdot}MeOH{\cdot}H_2O\}_n]$

Slow diffusion of solutions of ligand **2** in MeOH/1,2-$Cl_2C_6H_4$ and $Co(SCN)_2$ in MeOH in a sealed tube at room temperature resulted in the growth of crystals of $[\{Co(\mathbf{2})_2(NCS)_2{\cdot}0.67C_2H_4Cl_2{\cdot}MeOH{\cdot}H_2O\}_n]$. Elemental analysis of the bulk sample confirmed the same stoichiometry as that determined by X-ray diffraction using a single crystal selected from the bulk material. The complex crystallizes in the monoclinic space group $C2/c$, and Fig. 5a shows the asymmetric unit in order to define the atom labelling. Each tpy unit coordinates through the outer pyridine rings, leaving

atoms N2 and N5 unbound. The octahedral coordination sphere of Co1 is completed by bonds to atoms $N3^{i}$ and $N6^{ii}$ (Co1-$N3^{i}$ = 2.1695(16), Co1-$N6^{ii}$ = 2.1723(16), symmetry codes i = 2 – *x*, 1 – *y*, 1 – *z*; ii = $^{3}/_{2}$ – *x*, $-^{1}/_{2}$ + *y*, $^{3}/_{2}$ – *z*), and the Co-N bond angles are in the range 87.58(7) to 93.21(7)°. Pairs of cobalt atoms (Co1 and $Co1^{i}$) are bridged by two ligands to produce [2 + 2] metallomacrocyclic assembly motifs (Fig. 5b). Two such motifs (shown in red in Fig. 6a) form opposite sides of a [6 + 6] metallomacrocycle, and the latter are connected into a (6,3) net; (this net description uses the cobalt ions as nodes). Viewing the two-dimensional net along the crystallographic *b*-axis (Fig. 6b) reveals that the 4-HC≡CC_6H_4 substituents protrude above and below the sheet. Alkyne unit C23H23 is directed towards a phenyl ring[37] (Table 3) in a non-adjacent sheet. In contrast, alkyne C46H46 in involved in a CH...S contact (Table 3) involving a thiocyanate ligand in an adjacent sheet. There are additional CH...π_{alkyne} packing interactions (Table 3).

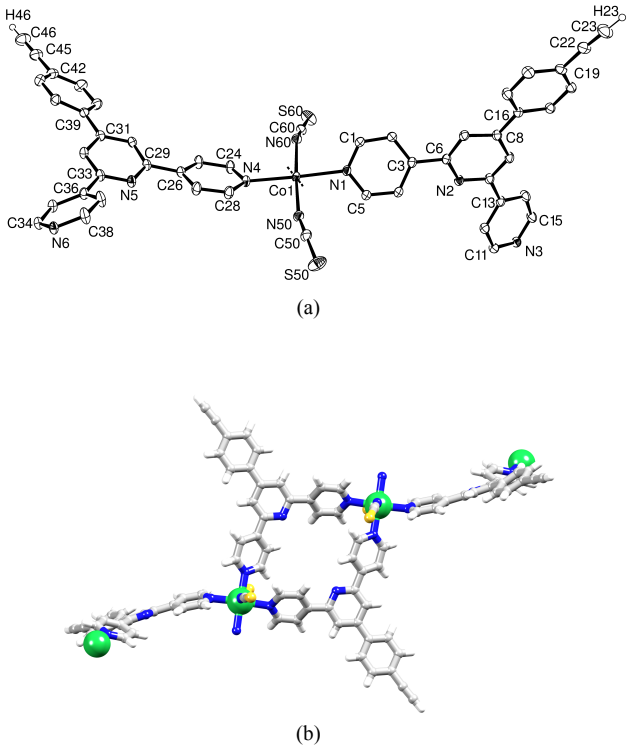

(a)

(b)

Fig. 5 (a) Asymmetric unit in [{Co(**2**)$_2$(NCS)$_2$·0.67$C_2H_4Cl_2$·MeOH·H_2O}$_n$] (ellipsoids plotted at 40% probability level; solvent molecules and H atoms except for C≡CH excluded). Hashed lines used to show the octahedral Co1 coordination geometry. Selected bond parameters: Co1-N1 = 2.1940(16), Co1-N4 = 2.1723(16), Co1-N50 = 2.0712(18), Co1-N60 = 2.0911(18), N50 C50 1.151(3), C50-S50 = 1.635(2), N60-C60 = 1.151(3), C60-S60 = 1.631(2) Å; C50-N50-Co1 = 165.19(18), C60-N60-Co1 =149.74(17)°. (b) A [2 + 2] metallomacrocyclic motif (see text).

Table 3. Intermolecular contacts in [{Co(**2**)$_2$(NCS)$_2$·0.67$C_2H_4Cl_2$·MeOH·H_2O}$_n$]. The symmetry code refers to the atom with the asterisk

D–H…A	H…A / Å	Symmetry code
C23H23...centroid of ring with C19*	2.87	$^{3}/_{2} - x, -^{1}/_{2} + y, ^{1}/_{2} - z$
C46H46... S60*	2.69	$x, -y, ^{1}/_{2} + z$
CH...π_{alkyne}		
C43*H43*...C46	2.87	$2 - x, -y, 2 - z$
C43*H43*...C45	3.19	$2 - x, -y, 2 - z$

It is noteworthy that both the independent 4'-phenyltpy domains in [{Co(**2**)$_2$(NCS)$_2$·0.67$C_2H_4Cl_2$·MeOH·H_2O}$_n$] are significantly twisted (Fig. 5a). The angles between the least squares planes of the pairs of rings containing atoms N1/N2, N2/N3, N2/C16, N4/N5, N5/N6 and N5/C39 are 34.20(9), 29.76(9), 14.29(9), 16.61(10), 40.87(10) and 20.90(10)°. Consequently, embraces of the 4'-phenyltpy domains which are often a dominant feature of the crystal packing of compounds containing these and related ligands,[38,39] are not important in [{Co(**2**)$_2$(NCS)$_2$·0.67$C_2H_4Cl_2$·MeOH·H_2O}$_n$].

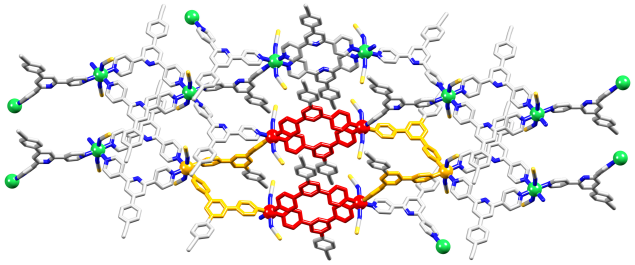

(a)

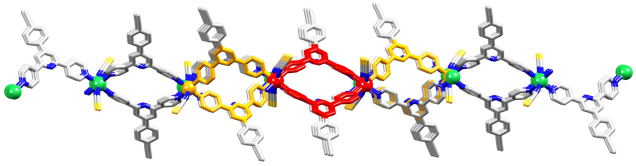

(b)

Fig. 6. (a) Part of one sheet in the solid state structure of [{Co(**2**)$_2$(NCS)$_2$·0.67$C_2H_4Cl_2$·MeOH·H_2O}$_n$] emphasizing the [6 + 6] metallomacrocyclic building block (orange and red) with the two component [2 + 2] macrocylic motifs in red. (b) The same unit as in diagram (a), viewed approximately along the *b*-axis showing the peripheral alkynylphenyl substituents.

[{Co(3)$_2$(SCN)$_2$·2MeOH}$_n$]

As discussed earlier, one aim in appending an imidazole domain is to explore the extent to which $NH_{imidazole}$...$N_{pyridine}$ hydrogen bonds contribute to the crystal packing of systems containing this ligand. Crystals of [{Co(**3**)$_2$(SCN)$_2$·2MeOH}$_n$] grew in a tube containing three layers: a MeOH/1,2-$Cl_2C_6H_4$ solution of **3**, an intermediate layer of MeOH and 1,2-$Cl_2C_6H_4$, and a final layer consisting of a MeOH solution of $Co(SCN)_2$. Multiple elemental analyses of the bulk sample are consistent with this being [{Co(**3**)$_2$(SCN)$_2$·MeOH·3H_2O}$_n$] rather than the crystallographically determined [{Co(**3**)$_2$(SCN)$_2$·2MeOH}$_n$].

Figure 7 illustrates the asymmetric unit in [{Co(**3**)$_2$(SCN)$_2$·2MeOH}$_n$] to define the atom numbering. Each of the two independent ligands **3** binds to the cobalt(II) ions through the outer pyridine rings, leaving pyridine atoms N4 and N9, and imidazole donors N6 and N11 non-coordinated. The octahedral coordination environment of Co1 is completed by bonds to atoms N5^{i} and N10^{ii} (2.1953(19) and 2.2228(10) Å, respectively, symmetry codes i = 1 – x, $^1/_2$ + y, $^1/_2$ – z, ii = x, –$^1/_2$ + y, $^1/_2$ – z). The tpy domain of the ligand containing atoms N8/N9/N10 is disordered, the outer rings severely so. The disorder has been modelled over two positions of occupancies 0.76 and 0.24; only the major occupancy sites are shown in Fig. 7 and the discussion of the structure is restricted to this ligand orientation. Each of the two independent ligands is highly twisted, just as is observed in the two coordination networks described above. The angles between the least squares planes of the pyridine rings including atoms N3/N4, N4/N5, N8/N9 and N9/N10 are 28.37(11), 26.55(11), 22.31(15) and 44.52(13)°. The deviation from planarity facilitates the assembly of a two-dimensional network, but as a consequence, tpy-tpy face-to-face π-interactions are not able to play a significant role in crystal packing (see below). The cobalt(II) nodes in [{Co(**3**)$_2$(SCN)$_2$·2MeOH}$_n$] are connected into a (4,4)-net and Fig. 8a depicts part of one sheet and highlights one [4 + 4] metallomacrocyclic building block. The assembly therefore resembles that in [{2Co(**1**)$_2$(NCS)$_2$·5H$_2$O}$_n$]. The imidazole substituents protrude from the upper and lower surfaces of the two-dimensional network (Fig. 8b). Each imidazole ring in one sheet is directed into a pocket formed by a tpy domain and thiocyanate ligands of the next sheet, and the packing interactions between adjacent sheets involve weak CH$_{imidazole}$…π, CH$_{pyridine}$…S and CH$_{imidazole}$…S contacts. Small cavities in the lattice are occupied by MeOH solvent molecules.

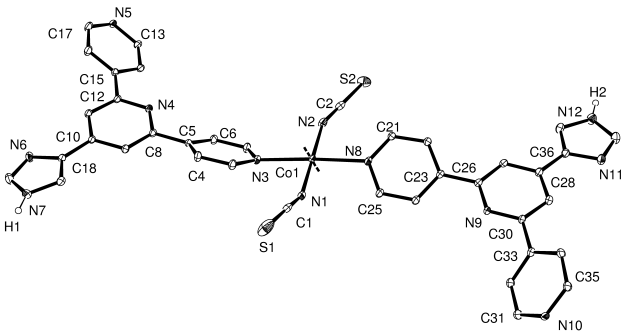

Fig. 7. The asymmetric unit in [{Co(**3**)$_2$(SCN)$_2$·2MeOH}$_n$] (ellipsoids plotted at 30% probability level; solvent molecules and H atoms except for imidazole NH are excluded). Only the major occupancy sites of the ligand containing N8/N9/N10 are shown (see text). Hashed lines emphasize that the overall coordination geometry at Co1 is octahedral. Important bond parameters: Co1-N1 = 2.063(2), Co1-N2 = 2.062(2), Co1-N3 = 2.2188(18), Co1-N8 = 2.2242(10), N1-C1 = 1.156(4), N2-C2 = 1.165(3), C1-S1 = 1.615(3), C2-S2 = 1.624(3) Å; Co1-N1-C1= 156.85(18), Co1-N2-C2 = 154.79(19)°.

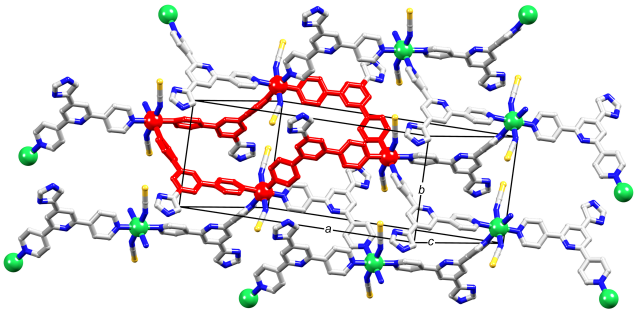

(a)

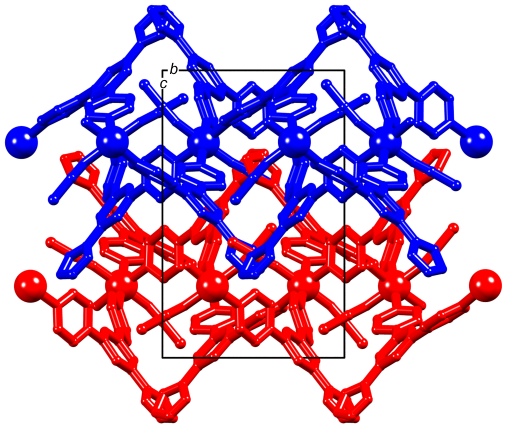

(b)

Fig. 8. (a) Part of one sheet in [{Co(**3**)$_2$(SCN)$_2$·2MeOH}$_n$] with one [4 + 4] metallomacrocyclic assembly motif coloured red. (b) A view down the *a*-axis showing interlocking of adjacent sheets. In both diagrams, Co atoms are shown in ball representation.

[{Co(4)(MeOH)$_2$(NCS)$_2$}$_n$]

Ligand **4** was selected for a preliminary investigation of complex formation using Co(NCS)$_2$ and a 3,2':6',3"-tpy metal-binding domain. We have previously described the assembly of a one-dimensional coordination polymer [{Cd(**5**)(OH$_2$)$_2$(ONO$_2$)(O$_2$NO)·H$_2$O}$_n$] in which ligand **5** is 4'-(4-dimethylaminophenyl)-4,2':6',4"-terpyridine.[8] This polymer contains approximately octahedral Cd(II) ions, with a *trans*-arrangement of *N*-donors that produces linear nodes. Polymer chains assemble into sheets with the NMe$_2$ unit sitting snuggly into the V-shaped cavity of the tpy unit of an adjacent chain. Sheets interact with one another through efficient face-to-face π-stacking of Phtpy domains.[8]

The reaction of ligand **4** with Co(SCN)$_2$ was performed using a layering technique in MeOH and 1,2-Cl$_2$C$_6$H$_4$ which yielded crystals within a month at room temperature. Crystals suitable for X-ray diffraction were selected, and structural determination confirmed a formulation of [{Co(**4**)(MeOH)$_2$(NCS)$_2$}$_n$]. Analysis of the bulk sample was consistent with a formulation of [{Co(**4**)(MeOH)$_2$(NCS)$_2$}$_n$]·0.33H$_2$O. The coordination polymer [{Co(**4**)(MeOH)$_2$(NCS)$_2$}$_n$] crystallizes in the orthorhombic space group *Pbca*, and the asymmetric unit is shown in Fig. 9. A bond to tpy donor atom N3^{i} (Co1–N3^{i} = 2.1658(16) Å, symmetry code i = $^1/_2$ – x, –y, –$^1/_2$ + z) completes the octahedral coordination sphere of Co1. Each

ligand **4** bridges between a pair of cobalt(II) centres and the *trans*-arrangement of the bridging ligands means that each metal ion acts as a linear node. The remaining four coordination sites are occupied by thiocyanate and methanol ligands (Fig. 9). Of the three possible conformations shown in Scheme 2, ligand **4** adopts a *trans,trans*-arrangement. Atom N2 of the tpy unit and N4 of the dimethylamino group remain non-coordinated. The tpy domain deviates from planarity, the angles between the least squares planes of the pyridine rings containing N1/N2 and N2/N3 being 24.01(9) and 29.02(19)°. In contrast, the phenyl ring is coplanar with the pyridine unit to which it is bonded (angle between the ring planes = 2.10(10)°). The curved profile of ligand **4** results in the propagation of undulating chains that follow the crystallographic *a*-axis (Fig. 10a).

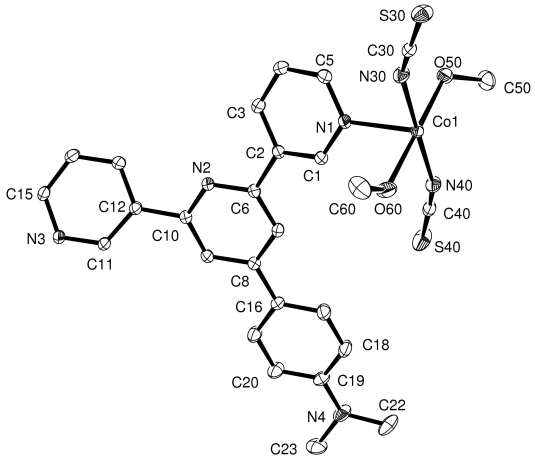

Fig. 9. The asymmetic unit in [{Co(**4**)(MeOH)$_2$(NCS)$_2$}$_n$] with ellipsoids plotted at 40% probability level and H atoms omitted. Hashed lines indicate the propagation of the polymer chain. Selected bond parameters: Co1-N1 = 2.1677(16), Co1-N40 = 2.0627(17), Co1-N30 = 2.0755(17), Co1-O60 = 2.1057(16), Co1-O50 = 2.1093(16), C19-N4 = 1.373(3), N4-C23 = 1.455(3), N4-C22 = 1.459(3) Å; C30-N30-Co1 = 154.56(16), C40-N40-Co1 = 160.31(17), N40-Co1-N30 = 178.30(7)°.

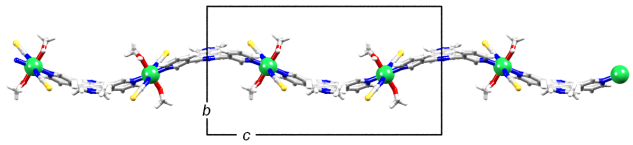

(a)

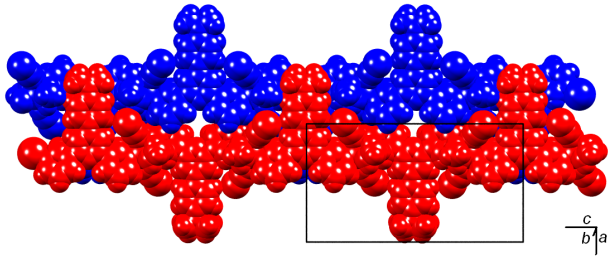

(b)

Fig. 10. (a) Part of one chain in [{Co(**4**)(MeOH)$_2$(NCS)$_2$}$_n$] running parallel to the *c*-axis. (b) Packing of two adjacent chains showing π-stacking of pairs of phenylpyridine units.

The chains in [{Co(**4**)(MeOH)$_2$(NCS)$_2$}$_n$] mesh together to give sheets, and chains in adjacent sheets associate through face-to-face π-stacking of centrosymmetric pairs of phenylpyridine units (inter-plane separation = 3.39 Å, $Ph_{centoid}\cdots py_{centroid}$ = 3.60 Å).[34] The relative orientations of the Phpy units render this a highly efficient interaction (Fig. 11a). The Me_2N substituent is accommodated in a shallow bowl-shaped cavity between the outer pyridine rings of the tpy unit of the adjacent ligand, and is involved in the close CH...π contact[40] shown in Fig. 11b (C23H23A...centroid of ring with N1^{ii} = 2.8 Å, symmetry code ii = 1 – *x*, –*y*, 1 – *z*). The offset arrangement of the Phpy units required for effective π-stacking precludes the NMe_2 group (red in Fig. 11) from engaging in CH...π interactions with both sides of the tpy domain (blue in Fig. 11).

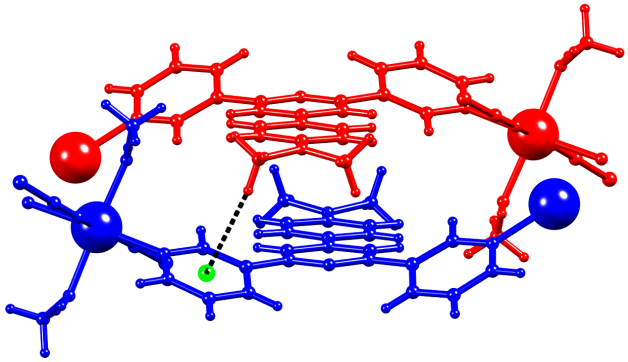

Fig. 11. Offset face-to-face π-stacking of centrosymmetric pair of phenylpyridine units in [{Co(**4**)(MeOH)$_2$(NCS)$_2$}$_n$], and the concomitant evolution of a CH...π interaction involving an H atom of the NMe_2 unit and pyridine ring containing atom N1^{ii} (symmetry code ii = 1 – *x*, –*y*, 1 – *z*).

A comparison of the one-dimensional coordination polymers formed between ligands **4** and **5** (3,2':6',3"- and 4,2':6',4"-tpy metal-binding domain, respectively) and a linear metal node, M, is instructive. The diagrammatic representation shown in Scheme 3 is based on the structures determined for [{Co(**4**)(MeOH)$_2$(NCS)$_2$}$_n$] (this work) and [{Cd(**5**)(OH$_2$)$_2$(ONO$_2$)(O$_2$NO)·H$_2$O}$_n$].[8] Although these polymers do not contain a common metal ion, both metal nodes are linear (N1-Co1-N3 = 178.35(7)° and N1-Cd1-N3 = 174.17(13)°, and the metal...metal separations along the chain are similar (Co...Co = 13.1339(7) Å and Cd...Cd = 12.472(3) Å). Despite the change in the substitution pattern on going from ligand **5** to **4**, Scheme 3 reveals similarities in the zig-zag topologies (distances between turning points and angle at each turning point). In practice, the change from a 4,2':6',4"- to 3,2':6',3"- substitution pattern on going from **5** to **4** is accompanied by a buckling of each tpy unit, and each undulating sheet in [{Co(**4**)(MeOH)$_2$(NCS)$_2$}$_n$] is replaced by a planar array in [{Cd(**5**)(OH$_2$)$_2$(ONO$_2$)(O$_2$NO)·H$_2$O}$_n$] (Fig. 12). This influences the manner in which chains in adjacent sheets interact. In both compounds, the recognition events between adjacent chains are π-stacking. However, whereas in [{Co(**4**)(MeOH)$_2$(NCS)$_2$}$_n$] this involves interactions between pairs of phenylpyridine units, stacking interactions in [{Cd(**5**)(OH$_2$)$_2$(ONO$_2$)(O$_2$NO)·H$_2$O}$_n$] are between pairs of pyridine rings. The resulting packing motif (Fig. 13) is also

observed $[\{Zn_2(OAc)_4(\mathbf{1})\}_n]$ and in analogous complexes containing 4'-(4-bromophenyl)-4,2':6',4"-terpyridine and 4'-(4-methylthiophenyl)-4,2':6',4"-terpyridine, each of which contains linear $\{Zn_2(OAc)_4\}$ nodes.[6,7] We propose that the switch from planar to undulating chains and sheets is a consequence of optimizing the π-stacking interactions.

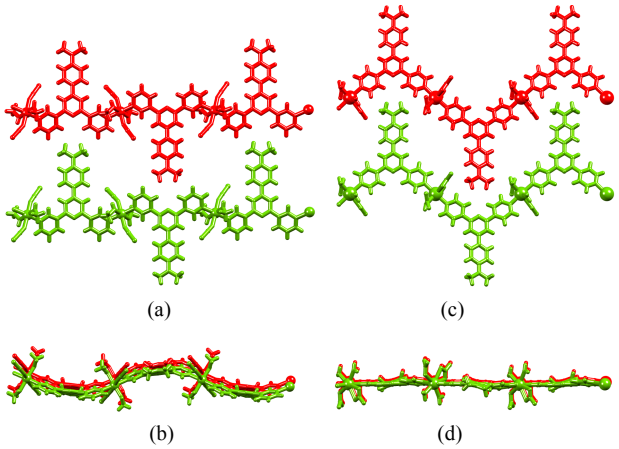

Fig. 12. Arrangements of two adjacent polymer chains in one sheet in (a)/(b) $[\{Co(\mathbf{4})(MeOH)_2(NCS)_2\}_n]$, and (c)/(d) $[\{Cd(\mathbf{5})(OH_2)_2(ONO_2)(O_2NO)\cdot H_2O\}_n]$.

s

Scheme 3. Comparison of the zig-zag chains defined by connectivity through linear metal nodes of the outer N-donors in ligands **4** (top) and **5** (bottom).

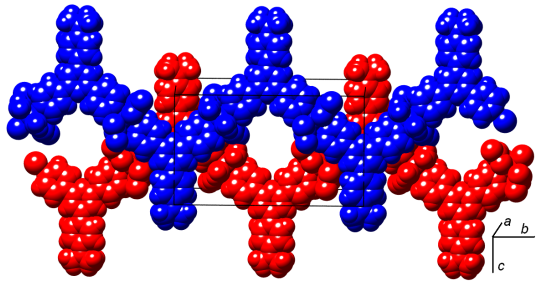

Fig. 13. Packing of two adjacent chains in $[\{Cd(\mathbf{5})(OH_2)_2(ONO_2)(O_2NO)\cdot H_2O\}_n]$.

Conclusions

The single crystal structures of the complexes $[\{2Co(\mathbf{1})_2(NCS)_2\cdot 5H_2O\}_n]$, $[\{Co(\mathbf{3})_2(SCN)_2\cdot 2MeOH\}_n]$ and $[\{Co(\mathbf{2})_2(NCS)_2\cdot 0.67C_2H_4Cl_2\cdot MeOH\cdot H_2O\}_n]$ reveal the assembly of (4,4) or (6,3) nets. These three coordination polymers contain 4'-substituted 4,2':6',4"-tpy ligands connected through *trans*-$\{Co(N_{tpy})_4(NCS)_2\}$ units (i.e. square-planar metal nodes), and reveal a common pattern: significant twisting of the tpy backbone facilitates network assembly and as a result, packing interactions are unable to utilize face-to-face π-stacking of tpy domains. In $[\{2Co(\mathbf{1})_2(NCS)_2\cdot 5H_2O\}_n]$, the coordinated ligands **1** do exhibit π-stacking of pairs of Phpy units between adjacent two-dimensional networks, but these stacking interactions are not as extensive as is present in related systems containing linear and bent nodes.

The one-dimensional coordination polymer $[\{Co(\mathbf{4})(MeOH)_2(NCS)_2\}_n]$ features undulating, zig-zag chains which are locked together to produce buckled sheets. A comparison between this assembly and the planar sheets observed in $[\{Cd(\mathbf{5})(OH_2)_2(ONO_2)(O_2NO)\cdot H_2O\}_n]$,[8] suggests that the structural modification is a consequence of optimizing face-to-face π-stacking interactions between adjacent 4'-(4-dimethylaminophenyl)-4,2':6',4"-terpyridine or 4'-(4-dimethylaminophenyl)-3,2':6',3"-terpyridine ligands. Whereas the rigidly defined orientation of the donor atoms in 4,2':6',4"-terpyridines predetermines the topology and topography of self-assembled one-dimensional systems, the use of the rotationally variable 3,2':6',3"-terpyridine allows access not only to one-dimensional systems as shown here, but also to materials with a higher dimensionality. This molecular diversity can be seen as an example of fuzzy logic[41] in the engineering of molecular materials. We are currently undertaking systematic studies of the variation in coordination polymer assemblies resulting from reactions of a given metal node and different isomers of 4'-substituted terpyridines.

Acknowledgements

We thank the Swiss National Science Foundation, the European Research Council (Advanced Grant 267816 LiLo), and the University of Basel for financial support. GZ thanks the Novartis Foundation, formerly Ciba-Geigy Jubilee Foundation for support.

Footnotes and references

Department of Chemistry, University of Basel, Spitalstrassse 51, CH-4056 Basel, Switzerland. Fax: +41 61 267 1018; Tel: +41 61 267 1008; E-mail: catherine.housecroft@unibas.ch; edwin.constable@unibas.ch

† CCDC ..... contain the supplementary crystallographic data for this paper. These data can be obtained free of charge from the Cambridge Crystallographic Data Centre via www.ccdc.cam.ac.uk/data_request/cif. See DOI:.....

74

1 M. Barquín, J. Cancela, M. J. González Garmendia, J. Quintanilla and U. Amador, *Polyhedron*, 1998, **17**, 2373.
2 G. W. V. Cave and C. L. Raston, *J. Supramol. Chem.*, 2002, **2**, 317.
3 L. Hou and D. Li, *Inorg. Chem. Comm.*, 2005, **8**, 190.
4 X.-Z. Li, M. Li, Z. Li, J.-Z. Hou, X.-C. Huang and D. Li, *Angew. Chem. Int. Ed.*, 2008, **47**, 6371.
5 E. C. Constable, G. Zhang, C. E. Housecroft, M. Neuburger and J. A. Zampese, *CrystEngComm*, 2009, **11**, 2279.
6 E. C. Constable, G. Zhang, E. Coronado, C. E. Housecroft and M. Neuburger, *CrystEngComm*, 2010, **12**, 2139.
7 E. C. Constable, G. Zhang, C. E. Housecroft, M. Neuburger and J. A. Zampese, *CrystEngComm*, 2010, **12**, 2146.
8 E. C. Constable, G. Zhang, C. E. Housecroft, M. Neuburger and J. A. Zampese, *CrystEngComm*, 2010, **12**, 3733.
9 B.-C. Wang, Q.-R. Wu, H.-M. Hu, X.-L. Chen, Z.-H. Yang, Y.-Q. Shangguan, M.-L. Yang and G.-L. Xue, *CrystEngComm*, 2010, **12**, 485.
10 J. Song, B.-C. Wang, H.-M. Hu, L. Gou, Q.-R. Wu, X.-L. Yang, Y.-Q. Shangguan, F.-X. Dong and G.-L. Xue, *Inorg. Chim. Acta*, 2011, **366**, 134.
11 J. Heine, J. Schmedt auf der Günne and S. Dehnen, *J. Am. Chem. Soc.*, 2011, **133**, 10018.

12 X.-Z. Li, X.-P. Zhou, D. Li and Ye-Gao Yin, *CrystEngComm*, 2011, **13**, 6759.
13 K.-R. Ma, F. Ma, Y.-L. Zhu, L.-J. Yu, X.-M. Zhao, Y. Yang and W.-H. Duan, *Dalton Trans.*, 2011, **40**, 9774.
14 J. Song, B.-C. Wang, H.-M. Hu, L. Gou, Q.-R. Wu, X.-L. Yang, Y.-Q. Shangguan, F.-X. Dong, G.-L. Xue, *Inorg. Chim. Acta*, 2011, **366**, 134.
15 E.C. Constable, G. Zhang, C.E. Housecroft and J. A. Zampese *CrystEngComm.,* 2011, **13**, 6864.
16 E. C. Constable, C. E. Housecroft, P. Kopecky, M. Neuburger, J. A. Zampese and G. Zhang, *CrystEngComm*, 2011, DOI: 10.1039/C1CE06024D.
17 F. Kröhnke, *Synthesis*, 1976, 1.
18 J. Wang and G. S. Hanan, *Synlett,* 2005, 1251.
19 J. Granifo, M. Vargas, M. T. Garland, A. Ibáñez, R. Gaviño and R. Baggio, *Inorg. Chem. Comm*., 2008, 11, 1388.
20 CSD version 5.32 with updates, Nov 2011.
21 F. H. Allen, *Acta Crystallogr., Sect. B*, 2002, **58**, 380.
22 B.-C. Wang, X.-L. Chen, H.-M. Hu, H.-L. Yao, G.-L. Xue, *Inorg. Chem. Comm*., 2009, 12, 856.
23 C. Liu, Y.-B. Ding, X.-H. Shi, D. Zhang, M.-H. Hu, Y.-G. Yin, D. Li, *Cryst. Growth Des.,* 2009*,* **9**, 1275.
24 Bruker Analytical X-ray Systems, Inc., 2006, APEX2, version 2 User Manual, M86-E01078, Madison, WI.
25 A. Altomare, G. Cascarano, G. Giacovazzo, A. Guagliardi, M. C. Burla, G. Polidori and M. Camalli, *J. Appl. Cryst.*, 1994, **27**, 435.
26 P. W. Betteridge, J. R. Carruthers, R. I. Cooper, K. Prout and D. J. Watkin, *J. Appl. Cryst*., 2003, **36**, 1487.
27 Stoe & Cie IPDS software v 1.26, Stoe & Cie, Darmstadt, Germany, 1996.
28 G. M. Sheldrick, Acta Crystallogr., Sect. A 2008, **64**, 112.
29 L. J. Farrugia, *J. Appl. Cryst*., 1997, **30**, 565.
30 I. J. Bruno, J. C. Cole, P. R. Edgington, M. K. Kessler, C. F. Macrae, P. McCabe, J. Pearson and R. Taylor, *Acta Crystallogr., Sect. B* 2002, **58**, 389.
31 C. F. Macrae, I. J. Bruno, J. A. Chisholm, P. R. Edgington, P. McCabe, E. Pidcock, L. Rodriguez-Monge, R. Taylor, J. van de Streek and P. A. Wood, *J. Appl. Cryst.*, 2008, **41**, 4646.
32 H. Walba and R. W. Isensee, *J. Org. Chem.*, 1961, **26**, 2789.
33 P. Koch, D. Schollmeyer and S. Laufer, *Acta Crystallogr., Sect. E,* 2009, **65**, o573.
34 C. Janiak, *J. Chem. Soc.*, *Dalton Trans.*, 2000, 3885.
35 M. Munakata, L. P. Wu and T. Kuroda-Sowa, *Adv. Inorg. Chem*., 1998, **46**, 173.
36 M. J. Zaworotko, *Chem. Commun*., 2001, 1.
37 S. Tsuzuki and A. Fujii, *Phys. Chem. Chem. Phys.*, 2008, **10**, 2584.
38 E. C. Constable, C. E. Housecroft, E. A. Medlycott, M. Neuburger, F. Reinders, S. Reymann and S. Schaffner, *Inorg. Chem. Commun.*, 2008, **11**, 805.
39 J. McMurtie and I. Dance, *CrystEngComm*, 2009, **11**, 1141.
40 M. Nishio, Y. Umezawa, K. Honda, S. Tsuboyama and H. Suezawa, *CrystEngComm*, 2009, **11**, 17.
41 L. A. Zadeh, *Inform. Control*, 1965, **8**, 338.